Available online at www.sciencedirect.com
SCIENCE DIRECT
Estuarine, Coastal and Shelf Science ■■ (2005) ■■■–■■■
ESTUARINE COASTAL AND SHELF SCIENCE
www.elsevier.com/locate/ECSS

Effect of channel bifurcation on residual estuarine circulation: Winyah Bay, South Carolina

Yong H. Kim [a,*], George Voulgaris [b]

[a] Department of Geological Sciences, University of South Carolina, Columbia, SC 29208, USA
[b] Department of Geological Sciences, Marine Science Program, University of South Carolina, Columbia, SC 29208, USA

Received 6 February 2004; accepted 11 July 2005

Abstract

The residual circulation pattern of Winyah Bay, the fourth largest estuary on the eastern coast of the US, is examined using stationary and shipborne current measurements during periods of low freshwater discharge. The estuary has a complex morphology with a single channel and narrow banks at the river entrance and the bay mouth, and a bifurcated channel system (main and western channels, respectively) in the middle part that appears to affect the residual circulation.

Overall, the upper (single channel morphology) and middle (dual-channel morphology) parts of the estuary exhibit a baroclinic residual circulation. The presence of bifurcated channels in the middle part of the estuary modifies the typical gravitational circulation. The near-bed landward-directed residual flow is stronger in the deeper main channel than the shallower western channel. This is the result of the fact that the magnitude of residual flow scales with the water depth of the channel and it is also influenced by the opposing patterns of channel alignment in the northern and southern junctions. Analytical modeling confirms that the observed residual currents in the upper and middle estuary are density-induced. In the lower estuary, residual flow is directed seaward throughout the water column of the channel while in the adjacent shoals the residual flow is directed landward, suggesting that in contrast to the upper and middle estuary, the residual flow near the mouth is barotropic, controlled by the tides and the channel-bank morphology.

Keywords: estuarine circulation; residual current; bifurcated channels; Winyah Bay; South Carolina

1. Introduction

Residual circulation dominates the flux of salt and other biological, chemical and geological materials in estuarine environments. Even though tidal current speed can be one order of magnitude greater than that of residual current, the latter plays an important role in net exchange of materials in solution or suspension. Understanding the processes that control patterns of residual circulation is a key element when considering long-term management of estuarine environments.

Estuarine residual currents have been attributed to well-known gravitational circulation, where a density gradient drives a seaward flow in the surface layer and landward currents near the bed (e.g., Pritchard, 1952; Hansen and Rattray, 1965). Recently, tidal pumping due to tidal asymmetry in turbulent mixing, which results from the strain-induced periodic stratification (Simpson et al., 1990), has also been suggested to cause residual currents (Jay and Smith, 1990b; Stacey et al., 2001). The relative importance of baroclinic (density gradient) and barotropic (tidal pumping) components

* Corresponding author.
E-mail address: ykim@geol.sc.edu (Y.H. Kim).

0272-7714/$ - see front matter © 2005 Published by Elsevier Ltd.
doi:10.1016/j.ecss.2005.07.004

on residual circulation depends on the particular characteristics of the estuary such as tidal range, freshwater input, and morphology. Circulation patterns are more complicated when the actual bottom topography is considered. Numerical work (Li and O'Donnell, 1997) has shown that for a simple v-shaped channel and narrow bank morphology and under barotropic forcing only, lateral variations in depth across the channel cause net landward flow over the banks balanced by a return seaward flow in the main channel. Furthermore, the same work showed that the intensity of the residual flow is controlled by the ratio between the depths on the shoal and in the channel. Experimental results from Chesapeake Bay (Valle-Levinson and Lwiza, 1995; Valle-Levinson and O'Donnell, 1996) demonstrated that when the barotropic forcing interacts with baroclinic processes, the residual circulation can be reversed (i.e., landward flow in the channels and seaward flow over the shoals). Furthermore, when the cross-section of the channel exhibits an asymmetric profile, then the location of the mean along-channel flow may be skewed toward the gentle-sloped side of the channel section (Friedrichs and Hamrick, 1996). When more than one channel is present then the channel's connectivity with the source of freshwater can control the patterns of residual circulation. For example, the North and South channels of the Columbia River estuary (Jay and Smith, 1990a,b) show different patterns of circulation. The North Channel is governed by seaward surface residual flow and landward bottom residual flow, while in the South Channel a seaward residual flow exists throughout the whole water column (Jay and Smith, 1990a).

Winyah Bay (WB), South Carolina, is the fourth largest estuary on the eastern coast of the USA in terms of discharge (Patchineelam et al., 1999) and is characterized by a complex geometry. WB is a coastal plain type estuary some 30 km long, extending from Georgetown, SC, to the Atlantic Ocean. The morphology of the estuary has a general S shape and it changes at various parts of the system (Fig. 1). The middle part of the estuary consists of bifurcated channels with different depths. The two channels merge at the upper and lower parts of the estuary. These locations of channel merge are hereafter called the northern and southern junctions and are bent to the west and east, respectively (see Fig. 1). A number of studies have been carried out in this area, but these have focused either on geochemistry (Goñi et al., 2003, in press), long-term sediment budget (Patchineelam et al., 1999), or suspended sediment dynamics (Patchineelam, 1999; Ramsey, 2000; Patchineelam and Kjerfve, 2004). Despite the importance of this area for navigational and environmental issues, no comprehensive study or data exist to-date that describe the general circulation pattern in this estuary.

The objective of this study is to present field hydrodynamic data describing the residual circulation of Winyah Bay. In particular, the role of the complex channel geometry and bifurcation on controlling residual circulation is examined. Spatially varying residual current pattern is revealed on the basis of hydrodynamic and hydrographic data collected during periods of low-river discharge conditions. A simple one-dimensional analytical model is applied to verify the effect of differences in water depth and bottom morphology on modifying residual circulation pattern in bifurcated channels. This work, although limited to low-river discharge conditions, establishes the general physical characteristics of the system and provides the background for any subsequent ecological or other environmental study in the area. Furthermore, the data provide a solid basis for the development and verification of numerical simulations that are underway but beyond the scope of this paper.

1.1. Study area

Winyah Bay (WB), South Carolina, is located approximately 70 km northeast of Charleston, SC. The estuary, seaward of the confluence of the Pee Dee and the Waccamaw Rivers, is 29 km long and encompasses a total area of 157 km^2, of which 92 km^2 are intertidal areas (South Carolina Sea Grant Consortium, 1992). WB has a narrow bay mouth and estuary head (1.2 and 2 km wide, respectively) but the middle, main estuary widens up to 7.2 km (Fig. 1). The bay is a microtidal system, subjected to semidiurnal tides with a mean tidal range of 1.4 m at the mouth and 1.0 m at the Sampit River entrance (NOS, 1995). There is a phase lag of approximately 2 h in the tide between the bay entrance and the head of the estuary at the confluence of the Pee Dee and the Waccamaw Rivers.

The total of mean freshwater input to WB is approximately 557 $m^3\,s^{-1}$ and is derived from a drainage area of 47,060 km^2. This discharge rate makes WB the fourth largest estuary on the east coast of North America, after St. Lawrence Waterway, Chesapeake Bay and Hudson River (Patchineelam, 1999). River discharge exhibits seasonal variability with the highest discharges occurring during late winter and early spring in response to snowmelt within the drainage area. The majority of the freshwater input is from the Pee Dee (~55%) and Little Pee Dee River (~20%), with smaller contributions from the Waccamaw (~8%), Black (~7%), Lynche (~7%), and Sampit (~1%) Rivers, which are typical low discharge coastal plain rivers (Patchineelam, 1999).

Sedimentation within the estuary is still extensive, although the construction of 20 dams on the Pee Dee River limits the delivery of eroded materials. A sediment budget study by Patchineelam et al. (1999) showed the input of sediments from the rivers reach up to 43×10^4 ton yr^{-1}. Three quarters of the delivered

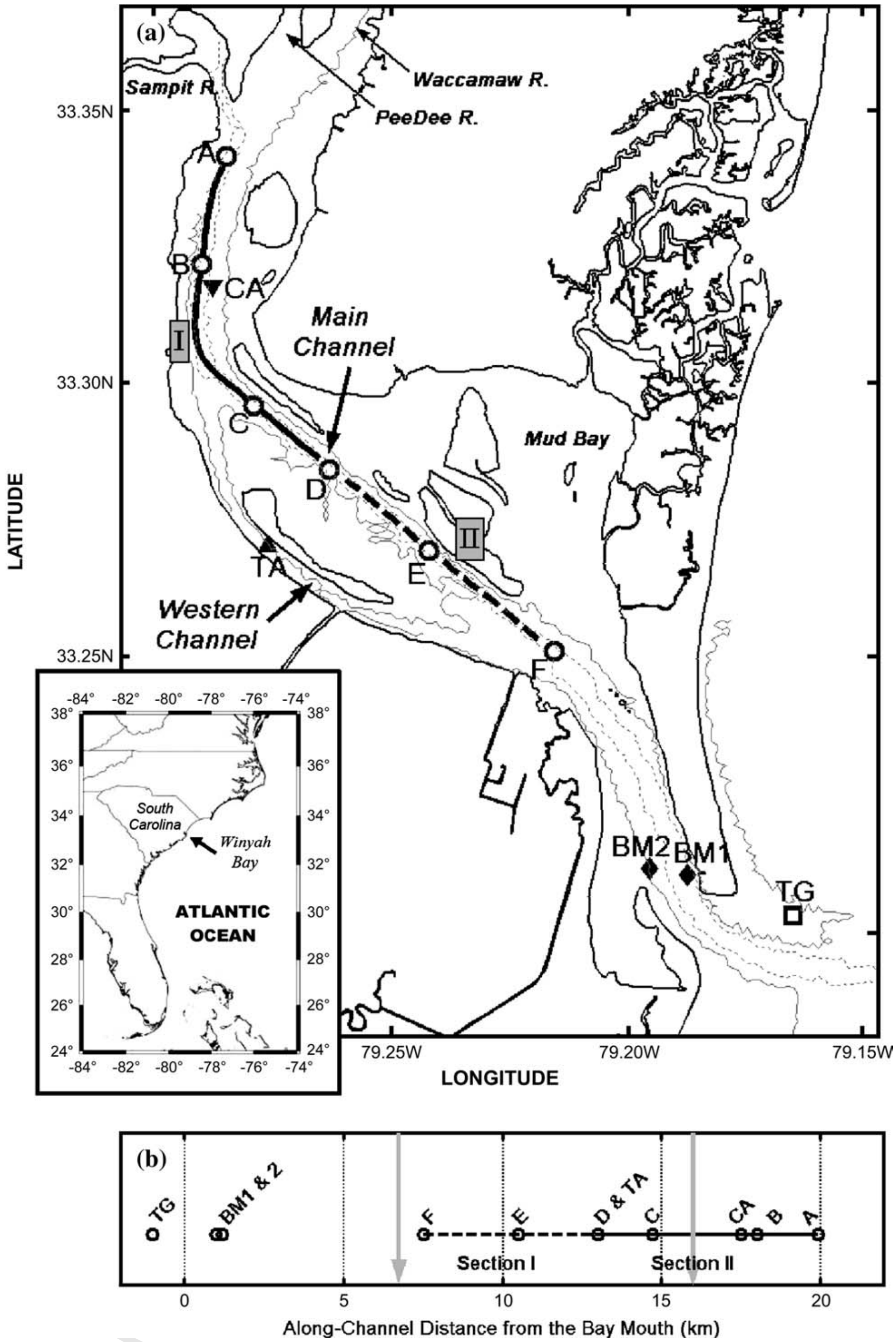

Fig. 1. (a) Map showing the study area, survey lines and locations of measurement stations. Transects I and II (solid and dashed lines, respectively) indicate shipborne ADCP surveys. CTD casts were carried out on stations A–F. Stationary current profile data were collected on locations CA, TA, BM1 and BM2 while a tidal gauge was installed on TG. The 3.5 and 6.5 m bathymetric contours are shown as solid and dashed lines, respectively. (b) Location of measurement stations as a function of along-channel distance from the mouth of the bay (BM). Gray arrows indicate the locations of western and main channel junctions (referred to as northern and southern junctions, respectively).

sediments are accumulating in the estuary, including channels, adjacent marshes or mud flats. Approximately 10.7×10^4 ton yr^{-1} of fine-grained sediment is dredged from the main navigation channel in order to maintain a shipping route to Georgetown Harbor (USACE, 1997).

Ramsey (2000) presented data showing that WB is characterized by a partially- and well-mixed estuary during high and low freshwater discharge period, respectively. The salinity front is located near the bay mouth during periods of high river discharge, whereas during periods of low discharge the salt wedge reaches up to 25 km upstream from the confluence of the Pee Dee and Waccamaw Rivers (South Carolina Sea Grant Consortium, 1992). The average depth of the bay is 4.2 m, with the deepest portions (~9 m) located in the artificially maintained shipping channel. The shallowest areas are located on its eastern flank of the middle estuary. Here, a large mud flat (Mud Bay) exists with water depths less than 0.5 m at low tide and extensive intertidal areas.

The morphology of the system is characterized by a single channel with narrow banks both at the river entrance (northern part) and the estuary mouth (Fig. 1). In the middle part (main estuary), the channel is subdivided into two tributaries: the main (located to the east) and the western channels, respectively. The main channel is dredged to 8.2 m below mean low water level while the western channel is semi-natural with a maximum water depth of 6 m. Both the northern and southern channel junctions are gently curved in opposite directions with west- and east-bent, respectively (see Fig. 1). As a result, the axes of the main channel in the middle and upper parts form an angle with each other in the vicinity of the northern junction area. Near the southern junction, the axes of the middle and lower part main channels are linearly aligned with each other.

At this juncture we should note that the present morphology of the estuary, as described above, is not the product of a natural flow system. Examination of the morphological development of the system, using 21 historical navigational charts covering the period 1854–1987 (http://historicals.ncd.noaa.gov/historicals/histmap.asp), revealed three development phases. The first phase (prior to 1877) corresponds to natural conditions without the influence of any anthropogenic modification. During this phase the estuary consisted of one deep channel (~6 m) in the upper part, three shallow (~4 m) channels in the middle part, and two distinctive (~5 m) channels in the lower estuary near the mouth. During the second phase (1877–1932), WB had one channel in the upper and lower part and two distinctive channels in the middle part of the estuary. The latter two channels had similar water depth of approximately 5 m. During the period 1948–1952, the main navigation channel in the center of the estuary was designed to be 28 km long, 8.2 m deep and 100 m wide (Conservation Foundation, 1980). This modification of the channels influences the present residual circulation pattern that is discussed in this paper.

2. Methodology

The data used in this study were collected during four different field measurement periods in 2001 and 2002. Each field campaign corresponded to different stages of the spring–neap tidal cycle (Fig. 2). Data corresponding to spring and neap tides were collected during the periods of September 9–13, and October 29–30, 2002, respectively. Another field campaign during October 3–6, 2001, coincided with transitional conditions from neap to spring. The most extensive field measurement campaign was conducted during the period of May 13–22, 2002, and included both transitional (neap–spring) and spring tide conditions. The Pee Dee River discharge, which represents 55% of the total freshwater discharge (see Section 1.1), ranged from 25.3 $m^3 s^{-1}$ in October 2001 to 190.9 $m^3 s^{-1}$ in October 2002 (see Fig. 2). These flow rates are 10% to 75% below the mean annual river discharge and represent low discharge conditions. During each field campaign shipborne and/or stationary data on currents, temperature, salinity, and water level were collected. Table 1 lists details of the field measurement program.

2.1. Shipborne data collection

The upper and middle section of the estuary (encompassing stations A–D; see Fig. 1) was surveyed during the periods of October 3–6, 2001, and May 13–17, 2002. The survey line (hereafter called Transect I) was limited to the main navigational channel due to the size of the vessel. Continuous mapping of the three-dimensional current structure along the channel axis was carried out using a ship-mounted, downward-looking RDI 1200 kHz acoustic Doppler current profiler (ADCP). The survey speed was less than four knots. The routine survey track consisted of sailing from station D to A with stops for CTD casts at each station and back to D without any stops at the stations. A full repetition of the survey track (i.e., from D to A and back to D) lasted 2–3 h. A total of 38 and 60 survey loops were conducted during October 2001 and May 2002, respectively. The first bin of the ADCP was located at 0.9 m below the water surface and the size of each bin was 0.25 m. One-second instantaneous current data were recorded on an on-board computer together with the ship's position and gyro data. These data were later averaged to 10-s mean velocities and corrected for ship movement and heading using the sensor's tilt meters and the ship's gyro output. Bottom-tracking correction was carried out using the data from the on-board differential GPS system.

The survey along the main channel of the middle estuary (hereafter called Transect II, encompassing stations from D to F; see Fig. 1) took place during May 20–23, 2002. The same instrumentation and procedure were used as described above. The survey loop, from F to D and back to F, was completed 47 times.

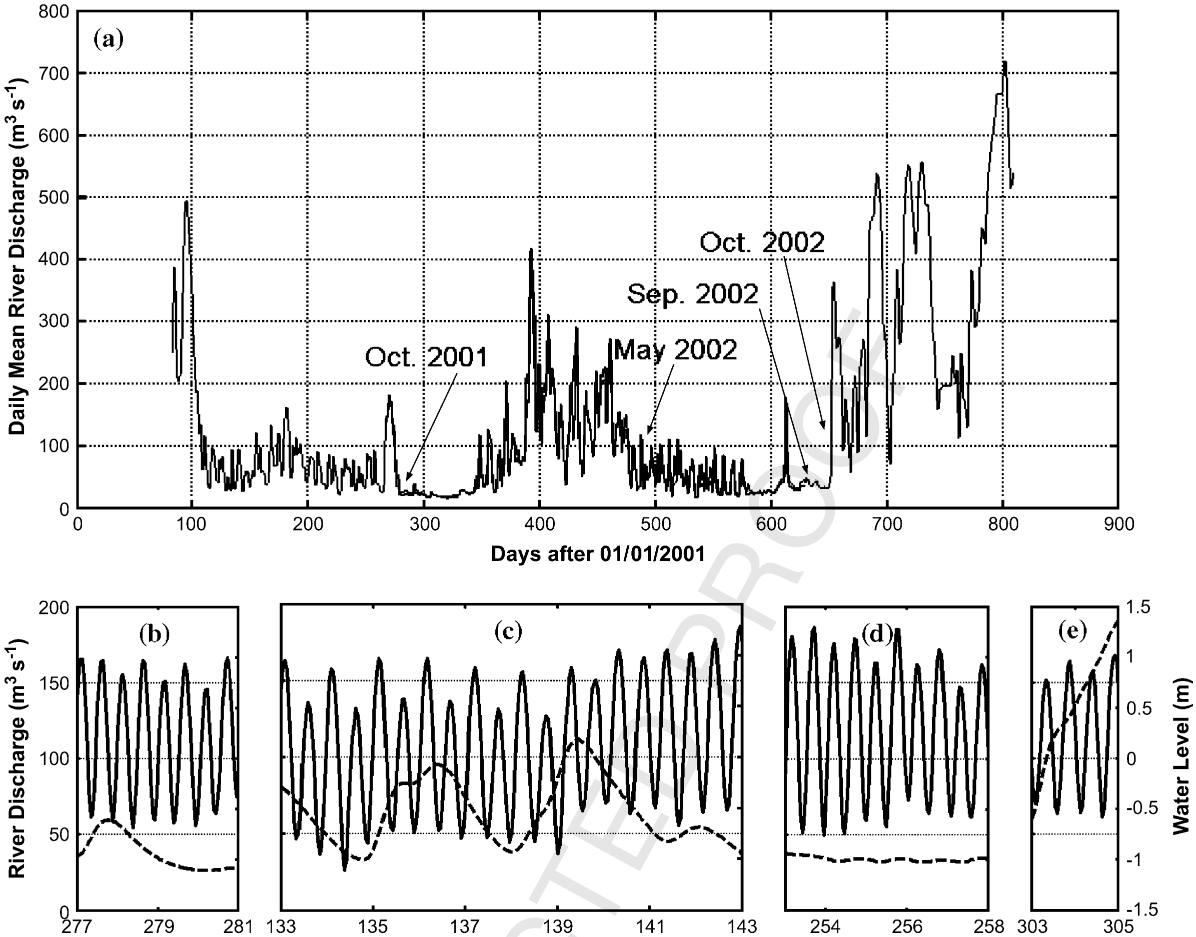

Fig. 2. Top: time-series of daily mean discharge of the Pee Dee River, which contributes 55% of freshwater discharge in Winyah Bay for the period of March, 2001 (day 82) to March 2003 (day 809). Bottom: time-series of hourly discharge for the Pee Dee River (dotted line) and water level for Charleston Harbor, SC for the data collection periods: (b) October 2001; (c) May 2002; (d) September 2002; and (e) October 2002. Horizontal axes represent year day of each year. (Discharge data from USGS station #02131000; water level data from, NOAA station #8665530).

2.2. Stationary data collection

During the period of May 13–22, 2002, current data were collected at two stations (CA and TA, respectively). Station CA (see Fig. 1) was located near the eastern margin of the navigation channel in the upper estuary, approximately 16.5 km from the bay mouth. A surface-mounted, downward-looking ADCP (RDI Workhorse 1200 kHz) was temporarily attached to a US Coast Guard navigational buoy. It recorded 6-min averaged current data every 10 min for 9 days (May 13–22, 2002). The first bin was located 0.75 m below the water surface and the bin size was set to 0.2 m. The bottom-tracking option was used to account for the movement of the buoy. However, it was found that the buoy tether line occasionally corrupted the near-surface bin data. Also, the echo return from the bottom was used to estimate water level variations on this site following the methodology described in Li et al. (2000).

During the same period, a bottom-mounted, upward-looking Doppler current profiler (2 MHz Nortek Aquadopp Profiler) was used to collect current data in the western channel (station TA, see Fig. 1). Current profiles were collected at elevations greater than 1.2 m above the bed with a bin size of 0.5 m. Two-minute averaged current velocities were recorded every 5 min. The instrument was originally installed at the center of the channel (water depth of ∼5 m), but it was dragged onto the shoal 1.5 days after deployment. The mean water depth on the shoal was around 1.5 m and therefore current observations on the shoal consist of only 1 or 2 bin measurements. A CTD (Sea-Bird SBE37) was also installed on the same tripod, measuring near-bed salinity and temperature at 1-min intervals.

Water level and temperature variation were collected at the mouth of the bay (location TG1, see Fig. 1) during the same period of May 2002. A self-recording tide gauge (RBR, XR-420 TG) was installed on the northern jetty of the mouth. These data were recorded every 6 min.

One-tidal-day (25 h) measurements of currents were conducted at each of the four stations (A–D) located in the main channel of the upper and middle estuary

Table 1
Description of measurement stations (for locations see Fig. 1), instrumentation used, periods and tidal conditions during period of data collection

Station	Instruments	Period	Location	Tidal regime
Transect I (A–D)	Ship-mounted ADCP	Oct. 3–6, 2001; May 13–17, 2002	Main channel in the upper and middle estuary	Transitional
Transect II (D–F)	Ship-mounted ADCP	May 20–23, 2002	Main channel in the middle estuary	Spring tides
A, B, C, D	Downward-looking ADCP	Sept. 9–13, 2002 (25 h for each station)	Main channel in the upper and middle estuary	Spring tides
CA	Downward-looking ADCP	May 13–22, 2002	Main channel in the upper estuary	Transitional/spring tides
TA-1	Upward-looking Aquadopp, CTD	May 13–14, 2002	Western channel bottom	Transitional
TA-2	Upward-looking Aquadopp, CTD	May 14–22, 2002	Shoal of the western channel	Transitional/spring tides
BM1	Downward-looking ADCP	Oct. 29–30, 2002 (25 h)	Channel bottom near the bay mouth	Neap tides
BM2	Downward-looking ADCP	Oct. 30–31, 2002 (25 h)	Shoal near the bay mouth	Neap tides
TG	Tide gauge	May 13–22, 2002	Bay mouth	Transitional/spring tides

during the period of September 9–13, 2002. A ship-mounted, downward-looking ADCP (RDI Workhorse Broadband 1200 kHz) recorded flow velocities continuously with a bin size of 0.25 m. These 25-h stationary data were used to verify the reliability of harmonic analysis on shipborne measured data, which were recorded at irregular time intervals.

Flow structure was also examined at two stations near the bay mouth, one in the channel and the other on the shoal, during each 25-h period in October 2002 (Table 1). Currents were measured continuously by a ship-mounted, downward-looking ADCP. The bin size was 0.25 m and the first bin was located at 0.9 m below the water surface. The first 25-h measurement period was carried out near the center of the main channel at a water depth of 9 m (station BM1, see Fig. 1). The boat was then relocated on the western shoal of the channel during the second day (station BM2, see Fig. 1). The mean water depth of station BM2 was approximately 4.5 m.

2.3. Data reduction and analysis

The three-dimensional current components from both shipborne and stationary ADCP measurements were converted to a channel-following orthogonal coordinate system with x and y being the across and along-channel axes, respectively. Positive signs represent up-estuary (flood conditions) and eastward/northeastward directed flows in the along- (y) and cross-channel (x) directions, respectively.

The survey lines along Transects I and II were subdivided into 100-m long segments. All current data collected within each segment were spatially averaged in the horizontal dimension. This spatial averaging procedure resulted in obtaining the current field with a 100 m and 0.25 m horizontal (along the main channel) and vertical resolution, respectively.

Residual currents for the along- and cross-channel components were estimated using a least-squares method that fits the raw data to the major tidal constituents (e.g., Geyer and Signell, 1990; Valle-Levinson and Lwiza, 1995). Although the short-term measurements (at most 9 days) are not long enough to resolve between the different semidiurnal (e.g., M2, S2, N2) or diurnal (K1, O1, S1, P1) tidal constituents (Valle-Levinson and Atkinson, 1999) the periods of the K1, M2 and M4 tidal constituents are used as representative of the general diurnal (di), semidiurnal (sedi), and quarterdiurnal (qdi) tidal oscillations, respectively. These periods were fitted to the time-series from each segment, and their amplitudes and relative phases were estimated as well as the residual flows as follows:

$$\begin{aligned}u(y,t) = {} & U_{\mathrm{o}}(y) + U_{\mathrm{di}}(y)\cos(\omega_{\mathrm{K1}}t - \psi_{\mathrm{di}}(y)) \\ & + U_{\mathrm{sedi}}(y)\cos(\omega_{\mathrm{M2}}t - \psi_{\mathrm{sedi}}(y)) \\ & + U_{\mathrm{qdi}}(y)\cos\big(\omega_{\mathrm{M4}}t - \psi_{\mathrm{qdi}}(y)\big) + u'(y,t) \quad (1)\end{aligned}$$

where u is the time-series of the current measured at each segment location y along the channel, U_{o} is the residual (subtidal) current at various segment locations (y), and U, ω and ψ are velocity amplitude, frequency and phase of each constituent. The last term u' represents signal from tidal constituents and other transient flows not resolved by the harmonic analysis. The tidally induced velocities predicted by the analysis explain more than 90% of the variance of the along-channel velocity component, while only 30–50% of the measured variance in the cross-channel direction was explained by the tidal signal. Hereafter, we focus mainly on the along-channel residual component. Significance intervals (95%) were estimated for the amplitudes of the residual currents.

The harmonic analysis was carried out for each bin throughout the water column and the results (amplitudes, phases and mean flows) were vertically averaged into two representative layers: surface (1–4 m below the surface) and bottom (4 m to bed). The depth of surface layer (i.e., 4 m) coincides with the average depth of the pycnocline and also represents the depth of the shoal margins.

3. Results

The results of this study are organized in two sections. Section 3.1 presents the analysis and results of a 9-day time-series from the stationary data. These include wind, water level, salinity, and tidal current data from May 2002. The analysis aims at describing general features of the study area and the effect of the coastal ocean in controlling dynamics within the estuary. The spatial variability of the residual currents is presented in Section 3.2.

3.1. Temporal variability of water level, salinity, and currents

The stationary measurements (for locations see Fig. 1) conducted during May 2002 provided a 9-day time-series of: (1) water level and temperature near the bay mouth (station TG); (2) salinity and temperature at the channel bottom in the middle part of the estuary (station TA); and (3) and tidal current data in the upper and middle estuary (stations CA and TA, respectively). These data were collected during a period when the tides were transitioning from neap to spring.

The water level signal recorded near the mouth is dominated by a semidiurnal tidal oscillation with a diurnal inequality (Fig. 3b). The tidal range varies from 1 to 1.5 m. A diurnal inequality is more pronounced during the first 5 days (transitional tide) of the time-series. The mean water level increases by approximately 0.5 m after calendar day 139. This increase was also observed in the water level data from the ADCP on station CA (upper part of the estuary; data not shown here). Furthermore, a similar increase was observed in sea surface elevation records from Charleston, SC, located some 70 km to the south of the study area (NOAA/NOS tide gauge #8665530, shown as gray line in Fig. 3b). Wind data measured by NOAA National Data Buoy Center (NDBC) on Folly Island (Station FBIS1) near Charleston show an abrupt change of wind direction from southwest to northeast at day 139 (Fig. 3a). This change created a coastal setup along the coast of SC that resulted in the observed elevated water levels inside the estuary, as it has been observed elsewhere (e.g., Wong and Garvine, 1984; Paraso and Valle-Levinson, 1996; Wong and Moses-Hall, 1998).

Near-bed salinity in the middle part of the estuary was recorded at station TA (Fig. 3c). The frame-mounted CTD was located in the middle of the western channel until day 135.7 (vertical dotted line in Fig. 3c), and then it was dragged on the shoal. A distinctive diurnal inequality was observed in the salinity variation when the sensor was located in the middle of the channel, especially during high tide (Fig. 3c). Salinity reached 22 and 29 during consecutive high tides, while the salinity during low tide ranged between 13 and 15. Salinity during high tide was lower on the shoal (days 135.7–139) than at the channel bottom (before day 135.7). However, salinity during low tide was in a similar range regardless of whether it was in the channel or on the shoal. Assuming that the salinity measured on the shoal is in similar range as that of the surface layer, the water masses are mixed well during low tide and rather stratified during high tide. The mean (subtidal) salinity on the shoal increased by approximately 3 after day 139 (see gray dashed line in Fig. 3c), which corresponds to the period of mean water level increase. During the same period, the mean water temperature at station TA and the bay mouth (black and gray lines in Fig. 3d, respectively) also decreased from 25 to 21 °C. Both the increase in salinity and decrease in temperature are supported by the notion of open ocean water of higher salinity and lower temperature being introduced in the estuary in response to the coastal setup.

Time-series of surface and near-bed current velocities from station CA at the upper part of the estuary are shown in Fig. 3. In the surface layer, the current speed reached 80 and 90 $cm\,s^{-1}$ during flood and ebb, respectively (Fig. 3e). The bottom currents reached no more than 70 $cm\,s^{-1}$ during maximum flood and ebb, which is approximately 20% lower than the surface current speed (Fig. 3f). Tidal asymmetry is more pronounced in the bottom layer than the surface layer. Both surface and bottom current velocities were generally higher during the first 3 days of the record and then decreased to 50 $cm\,s^{-1}$ during days 137–139. The magnitude of ebb flow was even smaller (less than 50 $cm\,s^{-1}$) at the bottom layer during days 139–140. This reduction of the magnitude of the ebb current, which coincided with periods of stronger flood current, was related to the coastal setup that occurred at day 139. After day 141, the magnitude of ebb current increased up to 70 $cm\,s^{-1}$ again.

The along-channel velocity data from the first bin (1.2 m above the bed) at station TA, which was located on the western channel, are shown in Fig. 3g. The data before day 135.7 (vertical dotted line in Fig. 3g) are representative of bottom flows at the channel thalweg that reached maximum speed of 70 and 60 $cm\,s^{-1}$ during flood and ebb, respectively. Ebb flow was dominant on the shoal (station TA, after day 135.7) reaching speeds of up to 50 $cm\,s^{-1}$ while current speeds during the flood never exceeded 40 $cm\,s^{-1}$.

3.2. Residual currents

In this section, the residual (subtidal) currents analysis for the data collected during the shipborne surveys of May 2002 and October 2001 are presented, followed by the results from the analysis of the current data collected at stations A, B, C, D, TA, CA, BM1 and BM2 (see Fig. 1).

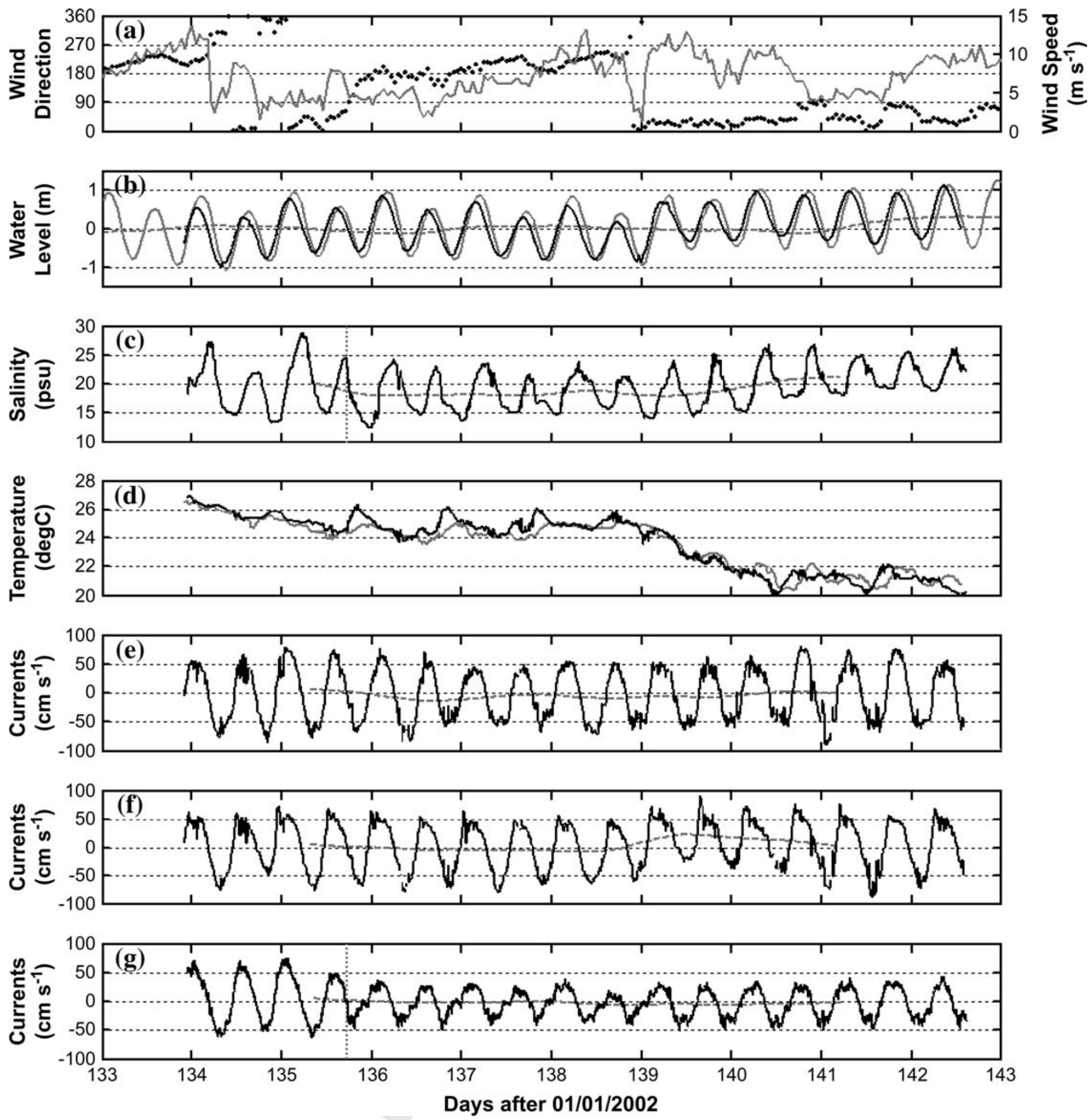

Fig. 3. Time-series of: (a) wind speed (gray) and direction (black) as measured at the NOAA/NDBC meteorological station located on Folly Island SC; (b) water level near the bay mouth (black line) and at Charleston Harbor (gray; data from NOAA/NOS station #8665530); (c) salinity measured at station TA in the western channel; (d) sea water temperature measured at station TA (black) and near the bay mouth (gray); (e) along-channel current velocity measured near the surface (2.1 m below the surface) in station CA; (f) along-channel current velocity measured near the bed at station CA; (g) bottom (1.2 m above the bed) current velocity observed at station TA in the western channel. Vertical gray dotted line represents the time of being dragged up to the bank. (Note: gray dashed line in (b), (c), (e), (f) and (g) represents 33-h filtered data).

The field experiment of May 2002 consisted of two periods: one was focused on the upper estuary (13–20 km from the bay mouth) and the other was for the middle estuary (7.5–12.5 km from the mouth; Fig. 4). Overall the residual current pattern resembles that of a density-driven circulation (i.e., landward bottom currents and seaward surface flow). At the 15 km location, which is near the northern junction of the main and western channels, the landward-directed residual flow extends throughout the water column. The strongest landward residual current (up to 33 cm s^{-1}) occurs near the bed at 14.5–16 km from the mouth. The magnitude of the bottom landward-directed current initially decreases toward the upper part of the estuary to almost zero, then increases again at a distance 19–20 km from the mouth. This increase of the landward-directed flow in the upper part of the estuary might be balanced by a seaward-directed flow in the adjacent shallow channel at the eastern side or the shallow parts of the estuary. The seaward-directed residual currents in the surface layer showed a peak of ~20 cm s^{-1} around the area 16 km from the mouth (Fig. 4). The surface residual currents range from 0 to 10 cm s^{-1} in the middle part of the estuary. The surface landward-directed flows at the 12 km and 15 km locations create zones of residual circulation convergence

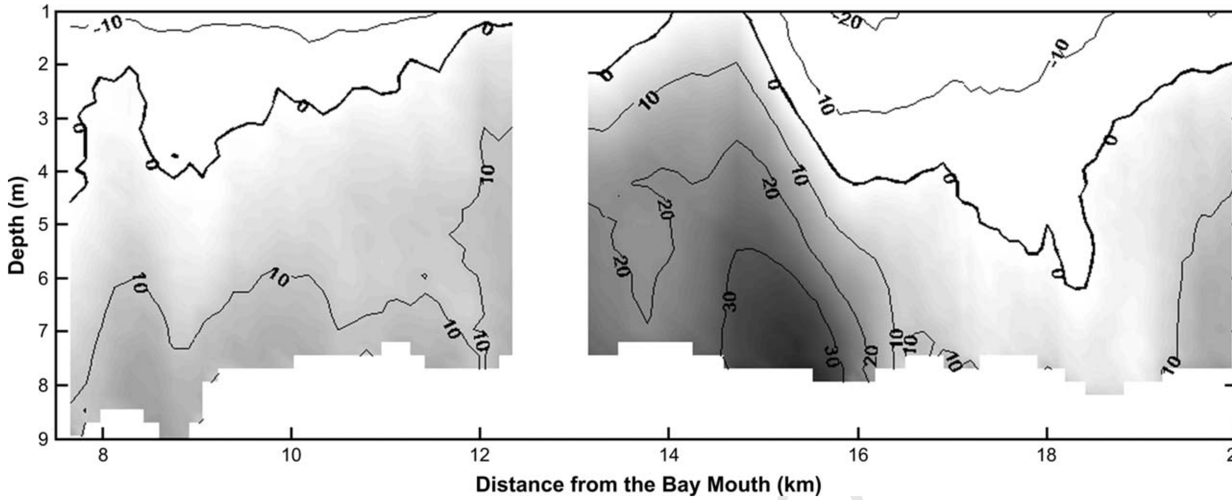

Fig. 4. Along-channel and vertical variability of the residual currents in the upper (13–20 km) and middle (8–13 km) parts of the estuary. Positive signs represent up-estuary or landward-directed flows.

and divergence on the surface layer (see Fig. 4). The convergence area occurs at the channel junction, which implies a possible net outflow to the western channel. The divergence occurs at location 13.5 km and might be related to the broad shallow area in the middle part of the estuary, including Mud Bay.

The consistency of the residual current circulation pattern observed during May 2002 is examined by comparing the results with measurements from other periods. The harmonic analysis results from the May 2002 data (Pee Dee River discharge of 65 $m^3 s^{-1}$) are first compared with those from October 2001 data (Pee Dee River discharge of 50 $m^3 s^{-1}$) and shown in Fig. 5. The vertically averaged residual currents from the two surveys show similar magnitudes and directions and almost identical spatial variability (solid and dashed lines in Fig. 5). In the upper and middle parts of the estuary, the bottom residual currents are always directed landward (black lines in Fig. 5). Landward-directed currents attain their minimum speed (<10 cm s^{-1}) in the region of 17–19 km from the mouth and their magnitude increases at both down- and up-estuary directions. The maximum landward-directed bottom residual current speed (~ 40 cm s^{-1}) occurs near the junction of the western and main channels (14.5–15.5 km from the mouth; Fig. 5). The surface residual currents in the upper part of the estuary are directed seaward with a maximum residual velocity of 20 cm s^{-1} at 16 km from the mouth of the bay (gray lines in Fig. 5), which corresponds to the location where the main and western channels merge together. Down-estuary from the junction of the two channels, some 14–15 km from the mouth, the along-channel surface residual current is directed landward with a speed of 10 cm s^{-1}. The surface

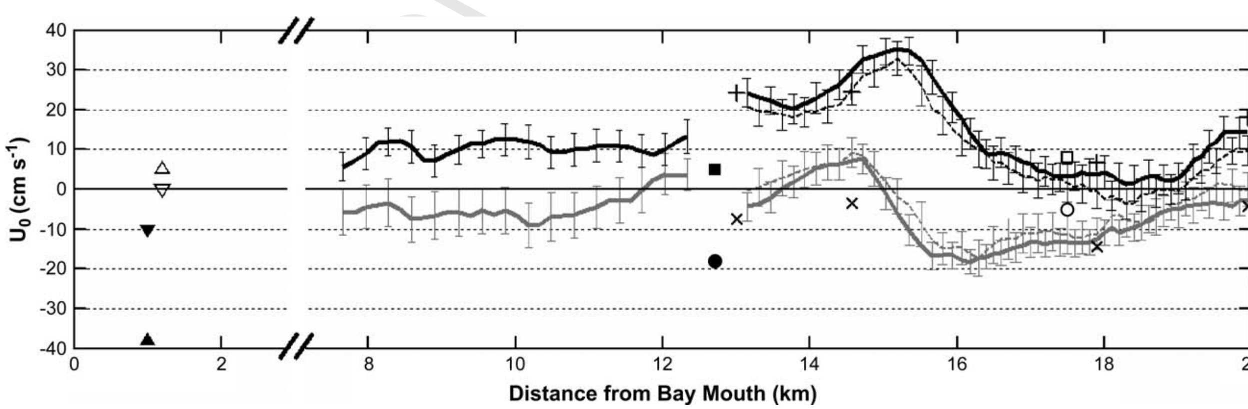

Fig. 5. Along-channel variability of the residual current velocities for surface (1–4 m) and bottom (4–8.5 m) layers. Solid and dashed lines represent data from the May 2002 and October 2001 surveys. Gray lines denote surface layer while black lines indicate conditions in the bottom layer. Error bars indicate 95% significance interval. Open circle and square represent surface and bottom current at station CA. Filled circle and square are results from surface and bottom current data at location TA. Symbols of x and plus denote surface and bottom residual currents on each CTD station during September 2002 (A–D). Upward-oriented and downward-oriented open triangles represent results from the surface and bottom layers in the navigation channel near the bay mouth. Filled triangles show flows over the shoal near the bay mouth.

residual current further downstream (7.5–11 km from the mouth of the bay) is directed seaward again with a speed of 5–10 cm s^{-1}.

Furthermore, residual currents were also estimated from the 25-h stationary measurements on stations A–D. These data were collected during September 2002, under low freshwater input condition (Pee Dee River discharge approximately 40 m^3 s^{-1}) and they agree well with those of May 2002 and October 2001 (see crosses in Fig. 5). This implies that the harmonic analysis of irregular-interval shipborne measured data is as reliable as that of stationary measured data.

Residual currents were also calculated from the 9-day long record at station CA during the same period as that of the shipborne measurements. For easy comparison, the estimated residual currents were averaged vertically for the surface (open circle) and bottom (open square) layers (Fig. 5). The results from this station show a good agreement with the pattern of residual currents established using the May 2002 shipborne data. A slight difference (~8 cm s^{-1}) was observed in the surface layer, which is attributed partially to the contamination of the data by the chain that connects the buoy to the anchor, and partially to the fact that the station was approximately 100 m away from the survey track of the shipborne measurement.

The residual circulation for the western channel was examined using the 36-h record from station TA. The surface layer shows relatively strong seaward flow up to 20 cm s^{-1} at 5 m above bed (filled circle in Fig. 5) and it decreases with depth. The bottom residual current is directed landward with a magnitude of 5 cm s^{-1} (filled square in Fig. 5). Analysis of the 8-day long current data collected on the shoal of the western channel revealed a seaward-directed residual current of 3–5 cm s^{-1} (not shown in the figure), which is smaller than that of the surface layer in the channel.

The pattern of residual flow near the mouth of the estuary is different from what has been described in the upper and middle parts of the estuary. The results from the bay mouth channel (station BM1) show a consistent seaward flow throughout the water column. The velocity of residual flow was larger in the surface layer (40 cm s^{-1}) and then decreased to 5 cm s^{-1} near the bed (see filled triangle in Fig. 5). However, the residual flow on the eastern shoal (station BM2) is directed landward with a magnitude of ~5 cm s^{-1} at the surface that decreases to zero near the bed (see open triangle in Fig. 5).

4. Discussion

When the density-induced gravitational current is considered to dominate the residual circulation pattern, the longitudinal momentum balance between tidally averaged horizontal pressure gradient (both barotropic and baroclinic) and vertical shear stress associated with the gravitational currents can be expressed as:

$$g\frac{\partial\eta}{\partial y} - \frac{g}{\rho_0}z\frac{\partial\rho}{\partial y} = -A_z\frac{\partial^2 u}{\partial z^2} \qquad (2)$$

where g is gravitational acceleration, η is tidally averaged surface elevation, ρ_0 is tidally and depth-averaged density, $\partial\rho/\partial y$ is tidally averaged horizontal density gradient which is assumed here to be independent of depth, A_z is eddy viscosity which is assumed to be a constant, u is the longitudinal component of the gravitational circulation, and y and z are positive to down-estuary and to the bottom, respectively. Assuming an estuary with a rectangular cross-section with flat bottom, then the continuity equation can be written as:

$$R = \int_0^H u\,\mathrm{d}z \qquad (3)$$

where R is the freshwater discharge divided by the width of the estuarine channel. The solution of Eqs. (2) and (3) assuming no wind stress at the surface and no bottom friction at the bed (i.e., $\partial u/\partial z = 0$ at $z = 0$ and $z = H$) is given by (Officer, 1976):

$$u(z) = \frac{gH^3}{24\rho_0 A_z}\frac{\partial\rho}{\partial x}\left[4\frac{z^3}{H^3} - 6\frac{z^2}{H^2} + 1\right] + \frac{3}{2}V_R\left[1 - \frac{z^2}{H^2}\right] \qquad (4)$$

where V_R is the vertically averaged freshwater runoff velocity per unit breath. The first and second terms in the right hand side of Eq. (4) represent the velocity induced by density gradient and freshwater runoff, respectively. The solution produces a vertical distribution of the residual velocity that is described by a third order polynomial, which represents opposite direction of surface and bottom residual flows. The magnitude is function of water depth, eddy viscosity, density, and horizontal density gradient.

Eq. (4) was fitted to residual current profiles for the upper and middle estuary collected during the May 2002 cruise. During this period the tidally- and depth-averaged density (ρ_o) was estimated to be 1010.8 kg m^{-3} while the value for $\partial\rho/\partial y$ was found to be 76.8×10^{-6} kg m^{-3}. Setting a mean channel depth of $H = 9$ m the least-square fitting analysis produced an eddy viscosity (A_z) value of 0.002 m^2 s^{-1} and a freshwater runoff velocity of 0.041 m s^{-1} (equivalent to river discharge of 124.1 m^3 s^{-1}) for the upper estuary (Fig. 6a). At this juncture it should be noted that the 48% overestimation of river discharge in the upper estuary (124.1 vs. the measured 64.5 m^3 s^{-1} at the Pee Dee River) by fitting the analytical models is due to the fact that the measured value represents only 55% of the total discharge (see Section 1.1) and it has been measured at a location 100 km upstream from the main estuary excluding approximately 45% of the watershed for Winyah Bay (Patchineelam, 1999). In a similar manner, Eq. (4) was fitted to the data from station TA (western channel, middle estuary, see Fig. 6b) setting $H = 6$ m and assuming the same mean density and density gradient values as before. The fitting procedure at this location produced an eddy viscosity (A_z) value of 0.001 $m^2\,s^{-1}$ and a freshwater runoff velocity of 0.018 $m\,s^{-1}$ (equivalent to river discharge of 19.9 $m^3\,s^{-1}$). The agreement between the model and the data is very good for both locations with the exception of the area near the surface in the western channel (Fig. 6b), where the measurements indicate stronger seaward-directed residual flows. This discrepancy is probably due to increased stratification in the upper layer and not well-mixed conditions as the model assumes. This can be the result of reduced tidal energy in the western channel (depth-averaged semidiurnal velocity amplitude 0.70 $m\,s^{-1}$ vs. 0.80 $m\,s^{-1}$ in the main channel) combined with increased flow of surface, fresh water which enters the western channel because of Coriolis and curvature effects (see below).

Application of Eq. (4) at station D, located in the main channel of the middle estuary does not agree with the measured vertical distribution of the residual flow at this site (see solid gray line in Fig. 6c). Considering that Eq. (4) assumes a rectangular cross-section for the channel while the study area at this location is dominated by the presence of broad shallow regions on the eastern side (Mud Bay, see Fig. 1) the disagreement between data and model results is not surprising. The cross-section area of shallow regions in both side of channel is approximately 4600 m^2, which is

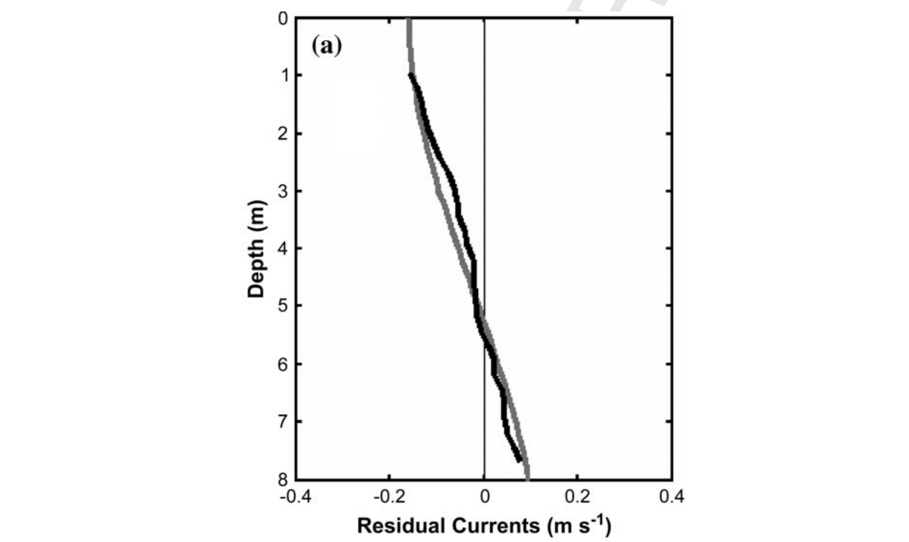

Fig. 6. Comparison between the analytical model results (gray line) and the observed data (black line) at: (a) upper estuary, station B; (b) western channel, middle estuary, station TA; and (c) main channel, middle estuary, station D. Solid and dashed gray line in (c) represent the model fits for rectangular (Eq. (4)) and triangular cross-section domain (Eq. (6)), respectively.

75% of total cross-section area. Wong (1994) suggested that a triangular cross-section is more reasonable approximation than a rectangular one for drowned river valleys where the cross-sections are characterized by deep channels in the central part with shallow shoals at both margins. Applying Wong's (1994) triangular cross-section ($H(x)=H_0(1-x/B)$, where H_0 is the maximum depth at the center ($=9$ m), x is the cross-channel coordinate, and B is half of the estuarine width, approximately 1800 m), the continuity Eq. (3) can be modified as:

$$R=\int_{-B}^{B}\int_{0}^{H(x)} u\,\mathrm{d}z\,\mathrm{d}x \tag{5}$$

Combining Eqs. (5) and (2) and assuming the same boundary conditions as before for Eq. (4), the solution for the vertical profile of the density-induced residual currents at the center of the channel ($x=0$) is:

$$u(z)=\frac{gH^3}{60\rho_0 A_z}\frac{\partial\rho}{\partial x}\left[10\frac{z^3}{H^3}-15\frac{z^2}{H^2}+1\right]+\frac{3}{2}V_\mathrm{R}\left[1-\frac{z^2}{H^2}\right] \tag{6}$$

The solution shown by Eq. (6) is applied to the station D data with $H=9$ m assuming a river discharge of $104.2\ \mathrm{m^3\,s^{-1}}$, which is equal to the difference of freshwater runoff obtained from the fit of Eq. (4) to the data from the upper estuary and western channel and shown in Fig. 6c as a dashed line. The A_z value that produced the best fit was $0.0008\ \mathrm{m^2\,s^{-1}}$ Following this analysis, the depth-averaged runoff velocity estimated is approximately $0.017\ \mathrm{m\,s^{-1}}$, which is slightly smaller than that estimated using Eq. (4) for the western channel ($0.018\ \mathrm{m\,s^{-1}}$). The fit between the model (Eq. (6)) and the measurement is significantly improved (see Fig. 6c) with the exception near the bottom layer where the observed values are lower than those predicted by the model. Although this could be attributed to frictional effects, application of the model (Eq. (2)) with a non-slip boundary condition did not fit the data. However, we believe that the disagreement between observation and model is attributed to the fact that the actual bottom topography at this location is not triangular in shape as the model assumes. Instead, the broad shallow regions at the surface are tapering rather abruptly at a depth of approximately 4 m and create a narrow channel of width varying between 200 and 100 m near the bed (i.e., regularly dredged area, navigational channel). At this point, it should be noted that the best-fit values of eddy viscosity obtained varied from 0.0008 in the upper to $0.002\ \mathrm{m^2\,s^{-1}}$ in the middle estuary; these values fall within the range of values reported in the literature (e.g., Geyer et al., 2000; Peters and Bokhorst, 2001) providing some confidence to our analyses.

From the scaling of the solutions (4) and (6) is clear that the magnitude of the residual current is proportional to the cube of the channel depth. It implies that the difference in water depth between the two channels in the middle part of the estuary can control the residual circulation pattern. The results from stations TA (western channel) and D (main channel) are compared with each other, as both stations are located equal longitudinal distance (13 km) from the bay mouth. The residual currents in both locations have the same direction near the bed and surface (landward and seaward, respectively). In terms of magnitude, however, the near-bed residual flow is 6 times stronger on station D than TA ($\sim 25\ \mathrm{cm\,s^{-1}}$ vs. $\sim 4\ \mathrm{cm\,s^{-1}}$; Fig. 6) while the difference in channel depth could explain only an increase by 2 or 3 times.

Flow pattern in the vicinity of the northern channel junction area (16.5 km from the bay mouth) is summarized in Fig. 7, which shows a complex vertical structure of instantaneous current vectors in three

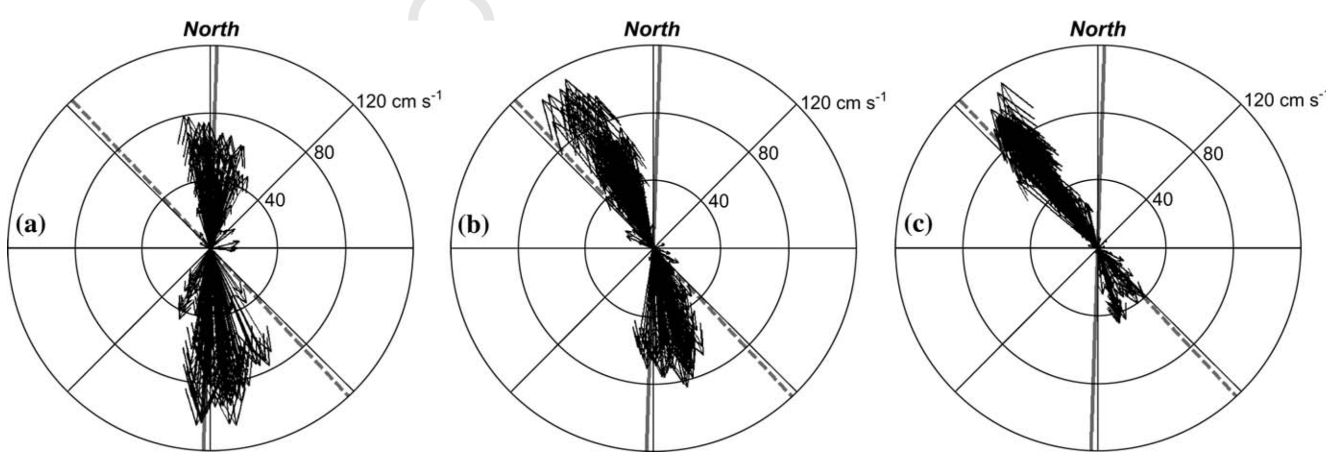

Fig. 7. Polar vector plot of instantaneous currents measured near the upper channel junction (16.5 km from the mouth of the bay) for: (a) surface layer (1–3 m below water surface); (b) mid-layer (3–5 m deep); and (c) bottom layer (below 5 m water depth). Solid and dashed gray lines indicate the orientation of the western (5° from north) and main (320°) channels in the middle part of the estuary, respectively.

layers: the surface (1–3 m below sea surface), middle (3–5 m below sea surface) and bottom layer (>5 m below sea surface). The direction of the surface current vectors coincides with the direction of the western channel axis (5° from north; Fig. 7a). On the other hand, bottom currents are aligned with the main channel axis of the middle estuary (320° from north; Fig. 7b). The middle layer corresponds to a transitional zone, where the ebb flow vectors are directed to the western channel but the direction of the current vectors during flood lie between the axes of the two channels. The observed layered flow implies that the surface water enters into the western channel while bottom water flow is confined to the main channel. The westward driving of this surface layer can be attributed to either the Coriolis or centrifugal force. In order to assess the relative importance of those two forcing simple scaling analysis is carried out. The Coriolis forcing scale is fU_o, where f is the Coriolis parameter ($=2.65 \times 10^{-5}\ \mathrm{s^{-1}}$) and assuming an along-channel residual velocity (U_o) of $0.1\ \mathrm{m\,s^{-1}}$ is estimated to be $2.65 \times 10^{-6}\ \mathrm{m\,s^{-2}}$. On the other hand, the curvature near the junction area gives rise to a centrifugal force, which can be scaled as U_o^2/R where R is the radius of curvature ($=1850$ m). Thus the estimated centrifugal forcing term is $5.39 \times 10^{-6}\ \mathrm{m\,s^{-2}}$, which appears to be of equal significance as the Coriolis force and it should be included in estimating estuarine circulation in systems with curvature and channel junctions similar to those of Winyah Bay.

The spatial variability of residual current vectors for the surface and bottom layers is presented in Fig. 8. Outflowing water in the surface layer is restricted to the western channel (Fig. 8a), while incoming water on the bottom of the upper estuary is confined to the deeper main channel (Fig. 8b). This segregation of the surface and bottom waters is attributed to the different orientation of main and western channels. The western and main channels of the middle estuary connect straight and obliquely to the upper estuary in the northern junction, respectively, which results in better connectivity between the upper estuary and the shallower western channel especially at the surface layer.

Although no measurements were taken near the southern junction area (6 km from the mouth of the estuary), it is hypothesized that the flow patterns occur as oppose to those of the northern junction. In the vicinity of the southern junction, the deeper main channel in the middle estuary is aligned parallel to that of the lower estuary, while the western channel links to the main channel at an angle. Thus, due to centrifugal

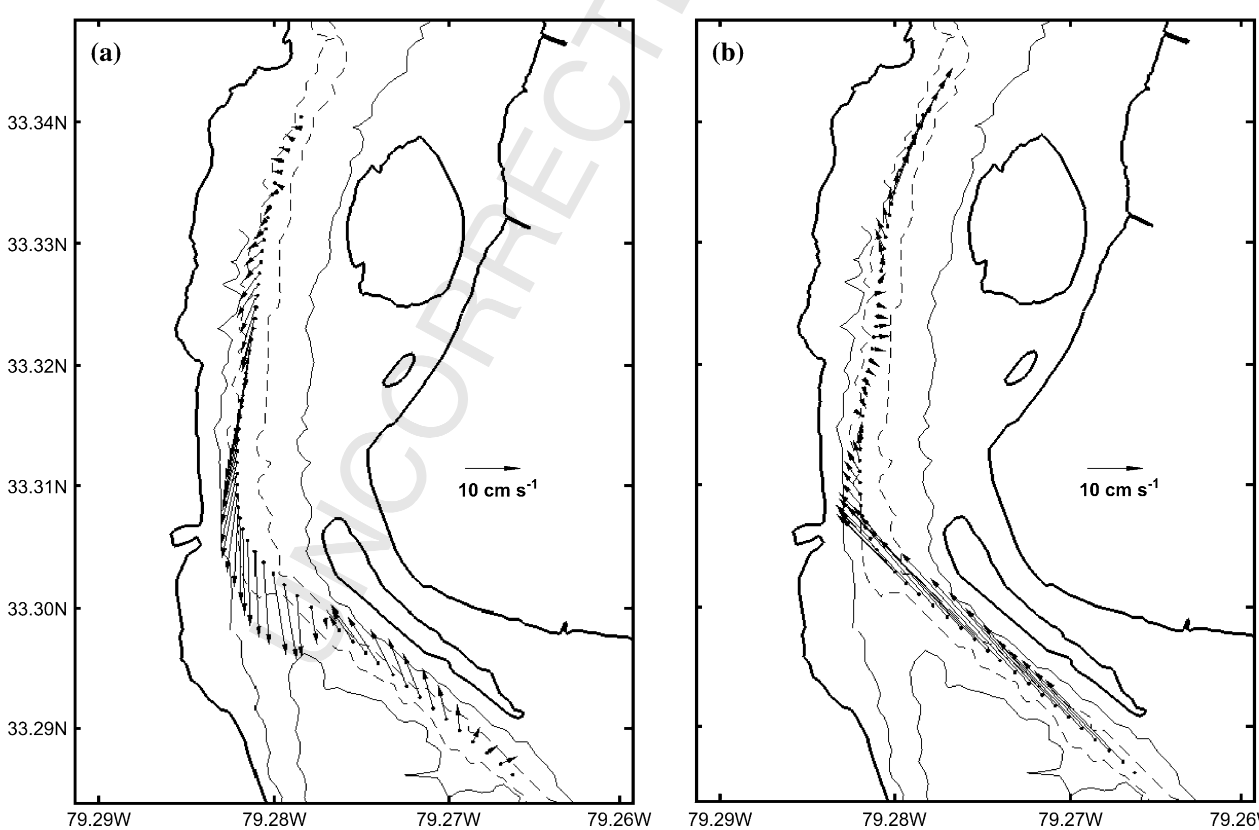

Fig. 8. Spatial variability of the residual current vector for the surface (a) and bottom (b) layers based on the May 2002 measurements in the upper and middle parts of the estuary. Note that the different directions near the channel junction. The solid and dashed lines represent the 3.5 m and 6.5 m contours, respectively.

force as mentioned above, most of the up-estuary directed seawater is expected to flow into the main channel rather than into the obliquely connected western channel. In addition to the effect of channel alignment the step-up at the entrance to the shallower western channel would now allow inflow of the saltier, denser bottom water mass.

Different tributaries exhibiting opposite residual currents have also been observed in the Columbia River estuary (Jay and Smith, 1990a,b), where landward- and seaward-directed residual currents were measured in the bottom layers of the North and South channels, respectively. Jay and Smith (1990a) attributed the observed patterns to the better connectivity of the South Channel to the up-river, which provided a better avenue for the freshwater to exit the system. Although both tributaries in the middle part of WB are connected to the up-river in contrast to the Columbia River, the different depths of the bifurcated channels as well as the different channel alignment at the northern and southern junctions give rise to the unique pattern of residual circulation in the middle part of WB.

Both bottom and surface residual currents in the channel-shoal system near the bay mouth are horizontally segregated (Fig. 5). A net outflow in the channel and inflow over the bank was observed at the WB mouth, which differs from the current circulation pattern observed and modeled in the lower Chesapeake Bay (Valle-Levinson and Lwiza, 1995; Valle-Levinson and O'Donnell, 1996). As shown by Li et al. (1998), tidally induced residual circulations have a seaward flow in the channel and a landward flow over the shoals, while density-driven residual flow is directed landward in the channel and seaward over the shoals. Thus, the residual flows in the vicinity of the mouth of the WB estuary appear to be predominantly controlled by the tidally induced (barotropic) component, especially during the low discharge condition presented in here.

Fig. 9 shows schematically the overall, synoptic residual circulation pattern for Winyah Bay during low freshwater discharge conditions. Gravitational circulation controls the residual currents in the upper and middle part of the estuary, while those in the lower part of the estuary are tidally driven. In particular, bifurcated channels with different depths modify the gravitational circulation in the middle part of the estuary, where stronger bottom and surface residual currents are observed in the deeper main and shallower western channel, respectively. This emerged circulation pattern was found to explain up-estuary local fluxes of vascular C_3 plants and estuarine algae with no significant contributions from marine phytoplankton

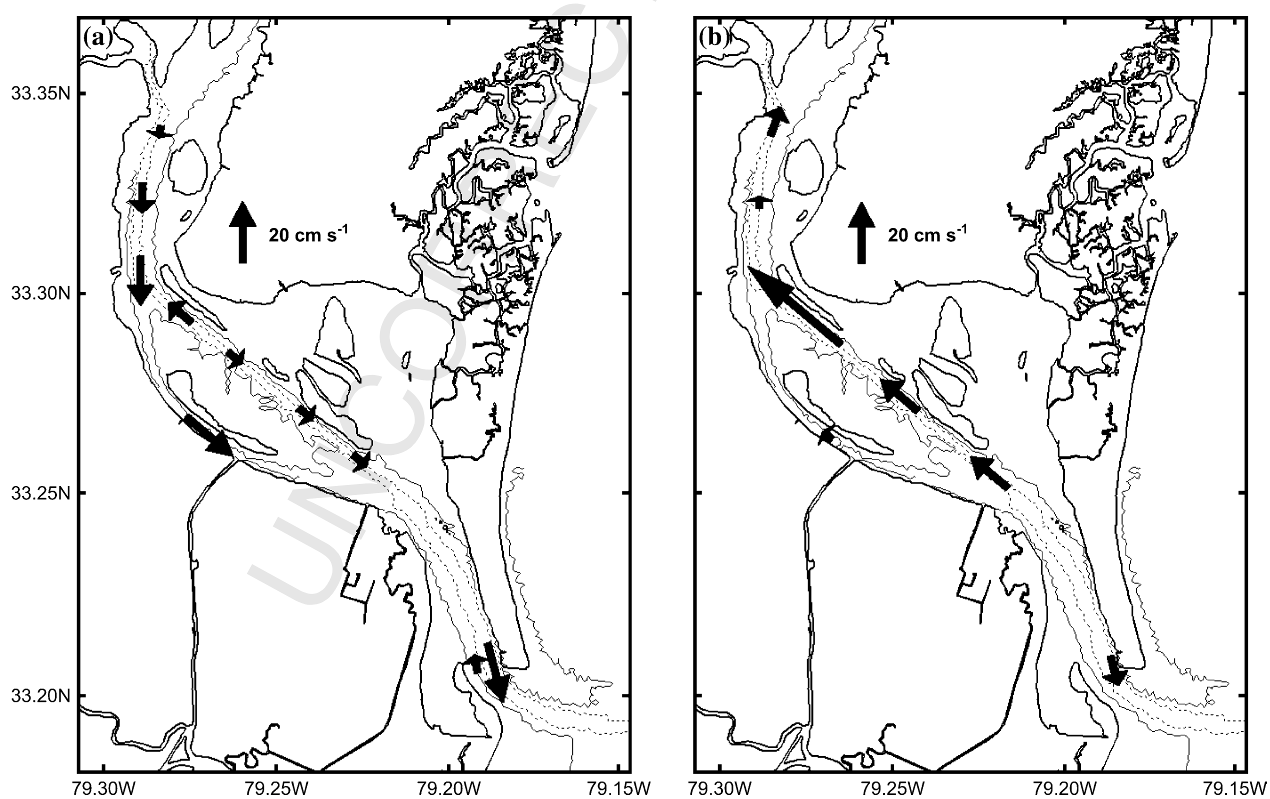

Fig. 9. Synoptic diagram showing the pattern of residual circulation in the Winyah Bay estuary for surface (a) and bottom (b) layers. The solid and dashed lines represent the 3.5 m and 6.5 m contours, respectively.

(Goñi et al., in press) and as such, this type of information is important in any ecosystem level modeling of the estuarine environment.

5. Conclusions

Residual circulation pattern in estuaries has been traditionally attributed to either baroclinic or barotropic processes. However, our study showed that under low freshwater discharge, different parts of an estuary can be under a different regime. The results of this study indicate that the upper and middle parts of the estuary are under a traditional gravitational circulation, where seaward flow in the surface layer balances with landward flow near the bed. In the lower estuary (i.e., bay mouth) the residual current is directed seaward throughout water column in the channel and landward over the shoals, suggesting that the residual flow is tidally induced. This difference is because the along-channel density gradient is relatively larger in the upper and middle estuary under low freshwater discharge conditions. The implication of these findings is that the relative importance of baroclinic and barotropic forcing on residual circulation can vary longitudinally and that local measurements at a single point might not be adequate in characterizing the estuarine environment.

The results of an analytical, one-dimensional, density-driven residual current model, which is based on balancing pressure gradient and vertical shear stress under well-mixed conditions, show good agreement with the observed data for both the upper and middle estuary, where baroclinicity controls residual circulation. Solutions assuming a rectangular cross-section (i.e., flat bed) provided best fit in areas with limited shallow areas around the channel (i.e., upper estuary and western channel), while a triangular channel cross-section provided a better approximation for the main channel of the middle estuary where broad shallow regions exist. These results are indicative of the sensitivity of the residual flows to channel morphology, and could be qualitatively parameterized as the ratio of cross-section area of the shallow region to that of the channel. When this ratio is large then the zero-velocity point of the residual in the main channel is moved toward the surface.

Analysis of the data showed that differences in channel depths in the middle of the estuary explain only partially the differences observed in the magnitude of the residual currents observed in the middle of the channels. Application of the analytical model revealed that bottom topography (channel dominated vs. channel-shoal system) is an equally important feature and should be accounted for. The discrepancy between the data and model results near the surface at the western channel indicates that there is additional fresh water input into the western channel due to differences in channel alignment at the bifurcation points (i.e., junctions). Opposing direction of curvature at northern and southern junctions results in opposite directed centrifugal forcing at each location. The centrifugal force is the same order of magnitude as the Coriolis force and both of them act toward the same direction steering fresh water into the western channel and salt water into the main channel.

The conclusions of this study are based on flow – morphology interaction for low discharge conditions and additional data and/or numerical simulations are required to extrapolate these finding to periods of high discharge. Nevertheless, a significant pattern has emerged and a solid database is presented that enables us to start evaluating important physical processes (like relative importance of curvature, Coriolis force and dual-channel morphology) and their importance in geochemical fluxes and carbon cycle studies in estuaries.

Acknowledgements

Financial support for this study was provided by an EPA grant (Grant #: R-82942402-0). Ship time onboard the R/V Ferrel was provided by NOAA through the NERR program. The captains and crew of R/V Ferrel and R/V Susan Hudson are thanked for their assistance. Drs. R. Styles and M. Goñi and are thanked for their help and comments. Dr. A. Valle-Levinson is acknowledged for providing some helpful insights in estuarine dynamics. Also the assistance of Ms. M. Cathey and all other graduate and undergraduate students of the University of South Carolina who helped during the field data collection are acknowledged. Finally, Dr. C.Y. Li and two anonymous reviewers are thanked for their critical and constructive inputs that helped to improve this manuscript.

References

Conservation Foundation, 1980. Winyah Bay reconnaissance study. Technical supplement, Washington, DC, pp. 40–80.

Friedrichs, C.T., Hamrick, J.M., 1996. Effects of channel geometry on cross sectional variations in along channel velocity in partially stratified estuaries. In: Aubrey, D.G., Friedrichs, C.T. (Eds.), Buoyancy Effects on Coastal and Estuarine Dynamics. American Geophysical Union, pp. 213–226.

Geyer, W.R., Signell, R., 1990. Measurements of tidal flow around a headland with a shipboard acoustic Doppler current profiler. Journal of Geophysical Research-Oceans 95 (C3), 3189–3197.

Geyer, W.R., Trowbridge, J.H., Bowen, M.M., 2000. The dynamics of a partially mixed estuary. Journal of Physical Oceanography 30, 2035–2048.

Goñi, M.A., Teixeira, M.J., Perkey, D.W., 2003. Sources and distribution of organic matter in a river-dominated estuary

(Winyah Bay, SC, USA). Estuarine, Coastal and Shelf Science 56, 1–26.

Goñi, M.A., Cathey, M.W., Kim, Y.H., Voulgaris, G. Sources and fluxes of suspended organic matter in an estuarine turbidity maximum region during low discharge conditions. Estuarine, Coastal and Shelf Science, in press.

Hansen, D.V., Rattray, M., 1965. Gravitational circulation in straits and estuaries. Journal of Marine Research 23, 104–122.

Jay, D.A., Smith, J.D., 1990a. Circulation, density distribution and neap–spring transitions in the Columbia river estuary. Progress in Oceanography 25 (1–4), 81–112.

Jay, D.A., Smith, J.D., 1990b. Residual circulation in shallow estuaries: 1. Highly stratified, narrow estuaries. Journal of Geophysical Research-Oceans 95 (C1), 711–731.

Li, C.Y., O'Donnell, J., 1997. Tidally driven residual circulation in shallow estuaries with lateral depth variation. Journal of Geophysical Research-Oceans 102 (C13), 27915–27929.

Li, C.Y., Valle-Levinson, A., Wong, K.C., Lwiza, K.M.M., 1998. Separating baroclinic flow from tidally induced flow in estuaries. Journal of Geophysical Research 103 (C5), 10405–10417.

Li, C.Y., Valle-Levinson, A., Atkinson, L.P., Royer, T.C., 2000. Inference of tidal elevation in shallow water using a vessel-towed acoustic Doppler current profiler. Journal of Geophysical Research-Oceans 105 (C11), 26225–26236.

NOS, 1995. Tide Tables 1996: High and Low Water Predictions, East Coast of North and South America, Including Greenland. NOS, 308 pp.

Officer, C.B., 1976. Physical Oceanography of Estuaries. John Wiley & Sons Inc, New York, 465 pp.

Paraso, M.C., Valle-Levinson, A., 1996. Meteorological influences on sea level and water temperature in the lower Chesapeake Bay: 1992. Estuaries 19, 548–561.

Patchineelam, S.M., 1999. Fine-grained sediment dynamics and budget: Winyah Bay estuary, South Carolina. PhD thesis, University of South Carolina, 190 pp.

Patchineelam, S.M., Kjerfve, B., Gardner, L.R., 1999. A preliminary sediment budget for the Winyah Bay estuary, South Carolina, USA. Marine Geology 162 (1), 133–144.

Patchineelam, S.M., Kjerfve, B., 2004. Suspended sediment variability on seasonal and tidal time scales in the Winyah Bay estuary, South Carolina, USA. Estuarine, Coastal and Shelf Science 59, 307–318.

Peters, H., Bokhorst, R., 2001. Microstructure observations of turbulent mixing in a partially mixed estuary. Part II: salt flux and stress. Journal of Physical Oceanography 31, 1105–1119.

Pritchard, D.W., 1952. Salinity distribution and circulation in the Chesapeake estuarine system. Journal of Marine Research 11, 106–123.

Ramsey, A.L., 2000. Physical processes controlling sediment transport in Winyah Bay, South Carolina. Master thesis, Boston college, 137 pp.

Simpson, J.H., Brown, J., Matthews, J., Allen, G., 1990. Tidal straining, density currents, and stirring in the control of estuarine stratification. Estuaries 13, 125–132.

South Carolina Sea Grant Consortium, 1992. Characterization of the physical, chemical and biological conditions and trends in three South Carolina estuaries: 1970–1985. Winyah Bay and North Inlet estuaries 2, 117 pp.

Stacey, M.T., Burau, J.R., Monismith, S.G., 2001. Creation of residual flows in a partially stratified estuary. Journal of Geophysical Research-Oceans 106 (C8), 17013–17037.

USACE, 1997. Dredged Material Management Plan, Preliminary Assessment. USACE, Georgetown, SC.

Valle-Levinson, A., Lwiza, K.M.M., 1995. Effects of channels and shoals on exchange in the lower Chesapeake Bay. Journal of Geophysical Research 100, 18551–18563.

Valle-Levinson, A., O'Donnell, J., 1996. Tidal interaction with buoyancy-driven flow in a coastal plain estuary. In: Aubrey, D.G., Friedrichs, C.T. (Eds.), Buoyancy Effects on Coastal and Estuarine Dynamics. American Geophysical Union, pp. 265–281.

Valle-Levinson, A., Atkinson, L.P., 1999. Spatial gradients in the flow over an estuarine channel. Estuaries 22 (2A), 179–193.

Wong, K.C., Garvine, R.W., 1984. Observations of wind-induced, subtidal variability in the Delaware Estuary. Journal of Geophysical Research 89, 10589–10597.

Wong, K.C., 1994. On the nature of transverse variability in a coastal plain estuary. Journal of Geophysical Research 99, 14209–14222.

Wong, K.C., Moses-Hall, J.E., 1998. On the relative importance of the remote and local wind effects to the subtidal variability in a coastal plain estuary. Journal of Geophysical Research 103, 18393–18404.